PHYSICAL REVIEW A **78**, 010304(R) (2008)

Detection of transverse entanglement in phase space

D. S. Tasca,* S. P. Walborn, and P. H. Souto Ribeiro
Instituto de Física, Universidade Federal do Rio de Janeiro, Caixa Postal 68528, Rio de Janeiro, RJ 21941-972, Brazil

F. Toscano
Fundação Centro de Ciências e Educação Superior a Distância do Estado do Rio de Janeiro, 20943-001 Rio de Janeiro, Brazil and Instituto de Física, Universidade Federal do Rio de Janeiro, Caixa Postal 68528, Rio de Janeiro, RJ 21941-972, Brazil
(Received 5 March 2008; published 8 July 2008)

Transverse entanglement between pairs of photons can be detected through intensity correlation measurements in the near and far fields. We show theoretically and experimentally that at intermediate zones, it is also possible to detect transverse entanglement performing only intensity correlation measurements. Our results are applicable to a number of physical systems.

DOI: 10.1103/PhysRevA.78.010304 PACS number(s): 42.50.Ex, 03.65.Ud, 03.67.Bg, 42.50.Xa

Detection and quantification of entanglement is essential for the development of many applications in the field of quantum information. Several tasks proposed to take advantage of the entanglement properties of quantum systems can be experimentally tested with photons produced from spontaneous parametric down-conversion (SPDC) [1]. This is a versatile system, since SPDC photons can be prepared in entangled states of many different degrees of freedom, such as polarization [2], time bins [3], orbital angular momentum [4], as well as transverse spatial variables [5,6]. The latter concerns correlations between the transverse components of the wave vectors of the signal and idler photons, which have been extensively studied and utilized in the past decade [7–9]. They arise due to the localization of the emission of photon pairs and the phase-matching conditions for the nonlinear interaction between the pump, signal, and idler fields. Even though the quantum nature of spatial correlations was already evident [10], the formal relationship with entanglement was demonstrated only a few years ago [5,6]. Transverse entanglement was detected through the violation of a nonseparability criterion [11,12], based on intensity correlation measurements performed in the near and far fields. Entanglement in continuous variables (CV) is a rich research subject, because several quantum-information tasks can be optimized using high-dimensional Hilbert spaces [13,14]. SPDC is a natural option for the experimental investigation of transverse spatial entanglement, which can be present in other quantum systems [15,16].

So far, CV transverse entanglement detection has been based on intensity correlation measurements performed in the near and in the far field [5,6]. An interesting entanglement "migration" effect was shown recently by Chan *et al.* [17], in which entanglement moves from the real to the imaginary part of the two-photon wave function during propagation. In order to be able to detect entanglement in this case, it would be necessary to perform phase-sensitive measurements [18].

In this Rapid Communication, we show theoretically and experimentally that it is always possible to detect entanglement by performing intensity correlation measurements, even outside near- and far-field zones. We demonstrate the connection between the variances of two observables and the variances of these same observables rotated in phase space. We encounter the conditions for which entanglement detection is possible with intensity measurements, and others for which it is impossible. This connection allows one to circumvent problems like the migration of entanglement [17] by performing proper phase-space rotations on the observables. Though we consider the particular case of propagation of transverse correlations of photon pairs, our results can be used to improve detection of entanglement in other CV systems.

Our approach is based on the propagation of the signal and idler fields using the formalism of the fractional fourier transform (FRFT), which is parametrized by the angle α [19]. The FRFT appears naturally in a number of physical systems and describes rotation in phase space. In particular, it is possible to completely describe the propagation of a light field through the order α of the FRFT. For instance, the field at the source is given by a FRFT of order $\alpha=0$, and the usual Fourier transform, associated with Fraunhoffer diffraction in the far field, is given by an FRFT of order $\alpha=\pi/2$. Free propagation can always be described in terms of an FRFT operation up to a quadratic phase term, which can be considered essentially unity in the near and far field [24]. In Ref. [5], as is customary, detection of entanglement was actually performed using lenses to obtain the intensity correlations in the near-field ($\alpha=\pi$) and far-field ($\alpha=\pi/2$). Likewise, any FRFT of order α can be implemented perfectly with lenses [19,20].

We consider the experimental arrangement sketched in Fig. 1(a), where signal and idler photons from SPDC are sent through FRFT systems of order α_s and α_i, respectively.

Following Ref. [17], we write the two-photon wave function at the source in position representation as

$$\langle \rho_s, \rho_i | \Psi \rangle = \frac{1}{(\pi \sigma_- \sigma_+)^{1/2}} e^{-(\rho_i + \rho_s)^2/4\sigma_+^2} e^{-(\rho_i - \rho_s)^2/4\sigma_-^2}, \quad (1)$$

where $|\Psi\rangle$ is the two-photon quantum state produced by SPDC, ρ_s and ρ_i are appropriate dimensionless position co-

*tasca@if.ufrj.br

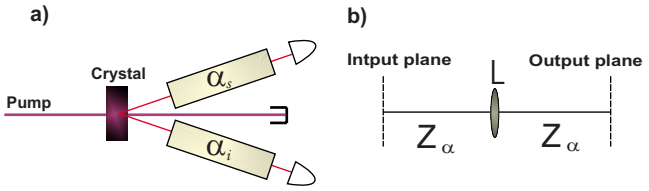

FIG. 1. (Color online) (a) Experimental setup. Boxes on signal and idler paths represent the optical systems used to perform FRFT of order α_s and α_i. (b) The optical lens system used to perform the FRFT [20]. L is a lens with focal length "f" and $z_\alpha = 2f\sin^2(\alpha/2)$.

ordinates in the source plane, and σ_+ and σ_- are independent functions of experimental parameters. Once the state at the source is taken to be approximately Gaussian, we only have to consider one spatial dimension. The two-photon wave function in wave-vector representation is

$$\langle q_s, q_i|\Psi\rangle = \sqrt{\frac{\sigma_+\sigma_-}{\pi}} e^{-\sigma_+^2/4(q_i+q_s)^2} e^{-\sigma_-^2/4(q_i-q_s)^2}, \qquad (2)$$

where q_s and q_i are transverse dimensionless wave-vector components at the source plane.

In order to detect entanglement of the state $|\Psi\rangle$, one must apply a separability criterion [11,12]. For example, defining the dimensionless operators $\hat{\rho}_\pm \equiv \hat{\rho}_i \pm \hat{\rho}_s$ and $\hat{q}_\pm \equiv \hat{q}_i \pm \hat{q}_s$ ($[\hat{\rho}_j, \hat{q}_k] = i\delta_{j,k} j$, $k = s,i$), the separability criterion of Duan, Giedke, Cirac, and Zoller (DGCZ) [11] establishes that if one of the two inequalities $\langle(\Delta\hat{\rho}_-)^2\rangle_\Psi + \langle(\Delta\hat{q}_+)^2\rangle_\Psi \geqslant 2$ or $\langle(\Delta\hat{\rho}_+)^2\rangle_\Psi + \langle(\Delta\hat{q}_-)^2\rangle_\Psi \geqslant 2$ is violated, then the state $|\Psi\rangle$ is nonseparable and therefore is entangled.

Using Eqs. (1) and (2), we have

$$\langle\Delta(\hat{\rho}_+)^2\rangle_\Psi = \sigma_+^2,$$

$$\langle\Delta(\hat{\rho}_-)^2\rangle_\Psi = \sigma_-^2,$$

$$\langle\Delta(\hat{q}_+)^2\rangle_\Psi = 1/\sigma_+^2,$$

$$\langle\Delta(\hat{q}_-)^2\rangle_\Psi = 1/\sigma_-^2, \qquad (3)$$

and we obtain

$$\langle(\Delta\hat{\rho}_-)^2\rangle_\Psi + \langle(\Delta\hat{q}_+)^2\rangle_\Psi = \sigma_-^2 + \frac{1}{\sigma_+^2}. \qquad (4)$$

The right-hand side (RHS) of Eq. (4) can be smaller than 2 for small σ_- and large σ_+. In the case of SPDC, this is readily achievable, as these two parameters are independent and experimentally accessible.

The variances in inequality (4) refer to position and momentum variables of the signal and idler fields in the source plane, which are related to the intensity distributions in the near and far field. It is well known that the propagation of a light field characterized by a FRFT is equivalent to a rotation of the transverse variables in phase space [19], given that these variables are properly adimensionalized [21]. The dimensionless operators transform as

$$\hat{\rho}_j \to \hat{\rho}_{\alpha_j} = \cos\alpha_j\hat{\rho}_j + \sin\alpha_j\hat{q}_j,$$

$$\hat{q}_j \to \hat{q}_{\alpha_j} = -\sin\alpha_j\hat{\rho}_j + \cos\alpha_j\hat{q}_j, \qquad (5)$$

where $j = s,i$. Therefore, it is possible to write the DGCZ inequality for rotated transverse variables of the fields, $\hat{\rho}'_- \equiv \hat{\rho}_{\alpha_s} - \hat{\rho}_{\alpha_i}$ and $\hat{q}'_+ \equiv \hat{q}_{\alpha_s} + \hat{q}_{\alpha_i}$, in terms of the variables $\hat{\rho}_-$ and $\hat{q}_+$ at the source [22],

$$\begin{aligned}\langle(\Delta\hat{\rho}'_-)^2\rangle_\Psi + \langle(\Delta\hat{q}'_+)^2\rangle_\Psi &= \frac{1+\cos(\alpha_i+\alpha_s)}{2}[\langle(\Delta\hat{\rho}_-)^2\rangle_\Psi + \langle(\Delta\hat{q}_+)^2\rangle_\Psi] \\ &+ \frac{1-\cos(\alpha_i+\alpha_s)}{2}[\langle(\Delta\hat{\rho}_+)^2\rangle_\Psi + \langle(\Delta\hat{q}_-)^2\rangle_\Psi] \\ &- \frac{\sin(\alpha_i+\alpha_s)}{2}[\langle\{\hat{\rho}_+,\hat{q}_+\}\rangle - 2\langle\hat{\rho}_+\rangle\langle\hat{q}_+\rangle]_\Psi \\ &+ \frac{\sin(\alpha_i+\alpha_s)}{2}[\langle\{\hat{\rho}_-,\hat{q}_-\}\rangle - 2\langle\hat{\rho}_-\rangle\langle\hat{q}_-\rangle]_\Psi. \qquad (6)\end{aligned}$$

Equation (6) shows that whenever $\alpha_i + \alpha_s (\mathrm{mod}\, 2\pi) = 0$, the sum of variances for the rotated variables coincides with the sum of variances for the variables at the source. This shows that, for any propagation of the signal field characterized by α_s, it is possible to find a propagation of the idler field α_i, so that intensity correlation measurement will violate the DGCZ inequality, in or out of the near and far field. We also note that Eq. (6) does not depend on the state [Eq. (1)] and is applicable to any bipartite continuous variable systems.

For states of the form (1), the last two lines on the RHS of Eq. (6) are zero. Then considering an entangled state satisfying $\langle(\Delta\hat{\rho}_-)^2\rangle_\Psi + \langle(\Delta\hat{q}_+)^2\rangle_\Psi = \sigma_-^2 + 1/\sigma_+^2 \leqslant 2$, a necessary condition to detect entanglement is

$$\cos(\alpha_i+\alpha_s) > \frac{S_1+S_2-4}{S1-S2} \geqslant 0, \qquad (7)$$

where we define $S_1 \equiv \sigma_+^2 + 1/\sigma_-^2$ and $S_2 \equiv \sigma_-^2 + 1/\sigma_+^2$. We note that for $\cos(\alpha_i+\alpha_s) = 0$, intensity correlation measurements never evidence entanglement, regardless of the state.

We have experimentally tested these conditions, using pairs of twin photons generated by SPDC in a 5-mm-long lithium iodate crystal ($LiIO_3$) with a cw diode laser oscillating at 405 nm, as shown in Fig. 1(a). Optical FRFT systems, such as the one shown in Fig. 1(b), were used in each of the down-converted fields. This system, with $z_\alpha = 2f\sin^2(\alpha/2)$, is able to implement a FRFT in the range $0 \leqslant \alpha < \pi$. For $\alpha \geqslant \pi$, we use a series of FRFT systems, respecting the additivity condition of maintaining $f' = f\sin\alpha$ [19] the same for each. To describe all FRFTs as rotations in the same phase space, we use dimensionless coordinates $\rho = \sqrt{k/f'}\,\bar{\rho}$ and $q = \sqrt{f'/k}\,\bar{q}$. In our experimental setup, $f' = 25/\sqrt{2}$ cm. Signal and idler photons were detected with single-photon counting modules and 10 nm full width at half-maximum bandwidth interference filters centered at 810 nm. Horizontal slits (100 μm) were mounted on translation stages and scanned vertically in steps of 50 μm to register the detection position. In all measurements, the "+" ("−") correlations were measured in all cases by scanning the detectors with equal steps in the same (opposite) directions.

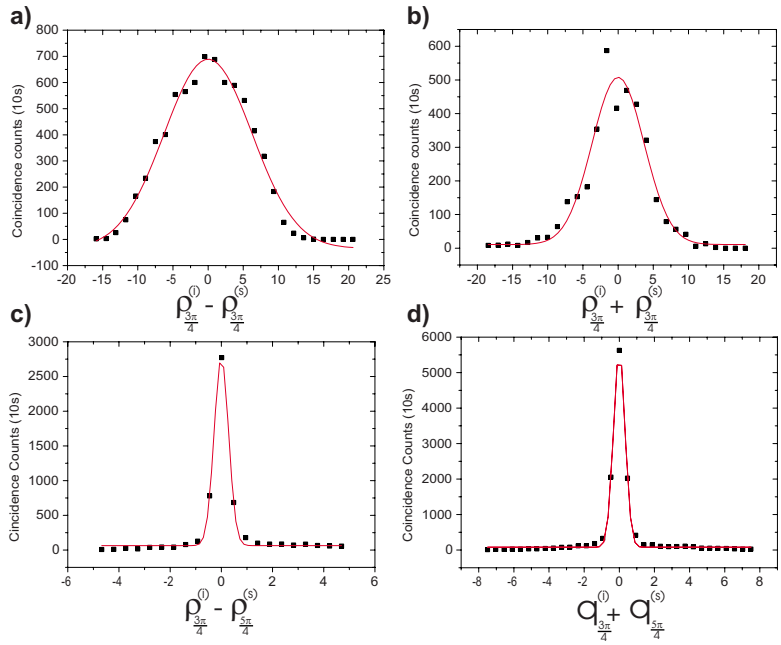

FIG. 2. (Color online) Measured coincidence counts and Gaussian curve fits. (a) $C(\rho^i_{3\pi/4}-\rho^s_{3\pi/4})$, (b) $C(\rho^i_{3\pi/4}+\rho^s_{3\pi/4})$, (c) $C(\rho^i_{3\pi/4}-\rho^s_{5\pi/4})$, and (d) $C(q^i_{3\pi/4}+q^s_{5\pi/4})$.

First, we measured the ρ_- and q_+ distributions at the source, using imaging ($\alpha_s=\alpha_i=\pi$) and Fourier transform ($\alpha_s=\alpha_i=\pi/2$) lens configurations [5]. The dimensionless variances were $\Delta^2(\rho_-)=0.93\pm0.01$ and $\Delta^2(q_+)=0.073\pm0.004$. Applying the DGCZ inequality, we obtain

$$\Delta(\rho_-)^2+\Delta(q_+)^2=1.00\pm0.01\leqslant 2, \tag{8}$$

indicating that the state is entangled.

Next, we measured the intensity correlations for the signal and idler fields at intermediate zones. We chose FRFT orders $\alpha_s=\alpha_i=3\pi/4$, so that $\cos(\alpha_s+\alpha_i)=0$, which does not satisfy the condition of Eq. (7). The coincidence counts $C(\rho^i_{3\pi/4}-\rho^s_{3\pi/4})$ and $C(\rho^i_{3\pi/4}+\rho^s_{3\pi/4})$ are plotted in Figs. 2(a) and 2(b), respectively. We obtain $\Delta^2(\rho^i_{3\pi/4}-\rho^s_{3\pi/4})=13.6443>2$ and $\Delta^2(\rho^i_{3\pi/4}+\rho^s_{3\pi/4})=39.1473>2$, which clearly indicates that these intensity correlations cannot be used to violate the DGCZ inequality. We also tested an intermediate zone configuration following the condition given by Eq. (7). We used three additive FRFT lens systems to perform an $\alpha_s=\frac{5\pi}{4}$ order FRFT on the signal field, while maintaining the $\alpha_i=\frac{3\pi}{4}$ order FRFT on the idler field, so that $\alpha_i+\alpha_s=2\pi$. Coincidence counts $C(\rho^i_{3\pi/4}-\rho^s_{5\pi/4})$ are plotted in Fig. 2(c), and the dimensionless variance is $\Delta^2(\rho^i_{3\pi/4}-\rho^s_{5\pi/4})=0.038\pm0.005$. Coincidence counts $C(q^i_{3\pi/4}+q^s_{5\pi/4})$, plotted in Fig. 2(d), were measured performing an inverse Fourier transform of the signal and idler fields at the planes of FRFT of order $\frac{5\pi}{4}$ and $\frac{3\pi}{4}$, corresponding to FRFT of orders $\frac{3\pi}{4}$ and $\frac{\pi}{4}$, respectively. The dimensionless variance is $\Delta^2(q^i_{3\pi/4}+q^s_{5\pi/4})=0.069\pm0.003$. With our experimental data, we are now able to verify entanglement at intermediate zones.

$$\Delta^2(\rho^i_{3\pi/4}-\rho^s_{5\pi/4})+\Delta^2(q^i_{3\pi/4}+q^s_{5\pi/4})=0.107\pm0.006<2. \tag{9}$$

The experimental values obtained in Eqs. (8) and (9) are not equal as expected from Eq. (6). This discrepancy can be explained by the experimental imperfections. It is difficult to characterize every source of experimental error and their precise effect on the measurement results. However, we notice that these imperfections contribute by broadening the coincidence distributions. In this respect, our measurement results are upper limits to the actual variances. To evaluate the expected variances, we characterized the initial state (1) at the source by measuring the width w of the intensity distribution of the pump beam. The dimensionless variance at the source is $\sigma_+^2=(4w^2)k/f'=47\pm2$. The dimensionless variance σ_-^2 is given by $\sigma_-^2=(k/f')0.455D/K=0.006$, where D is the length of the nonlinear crystal and K is the pump beam wave number [17]. With these values, we predict a violation of the DGCZ inequality: $\langle(\Delta\hat{\rho}_-)^2\rangle_{\text{th}}+\langle(\Delta\hat{q}_+)^2\rangle_{\text{th}}=0.027\pm0.001\leqslant2$, which is smaller than both experimental values (8) and (9). Therefore, it is clear that without the experimental imperfections, we should have observed even stronger violations for both cases. A possible imperfection is the error in lens positioning. The effect of this type of imperfection can be estimated by calculating the propagation through the different lens systems in each field [19] and including a 1% error in z for all lens systems. Taking the worst case scenario, we obtain the following predictions for each variance: $\Delta^2(\rho^i_{3\pi/4}-\rho^s_{5\pi/4})_{\text{th}}=0.09$ and $\Delta^2(q^i_{3\pi/4}+q^s_{5\pi/4})_{\text{th}}=0.04$, $\Delta^2(\rho_-)_{\text{th}}=0.84$ and $\Delta^2(q_+)_{\text{th}}=0.03$. These variances are much closer to the experimental values. Thus, considering small experimental imperfections, the theoretical prediction agrees with both Eqs. (8) and (9), as expected from Eq. (6).

Let us now discuss the application of these results to a situation similar to that of Ref. [17], in which it is shown that the transverse intensity correlations decrease as the field propagates, and then are recovered again in the far field. For a certain propagation distance, the DGCZ or similar inequal-

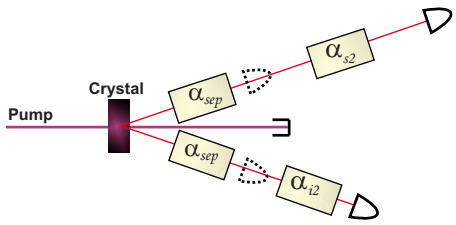

FIG. 3. (Color online) Both signal and idler fields propagate through lens systems that implement a FRFT of order $\alpha_{\mathrm{sep}}=\tan^{-1}(\sigma_+\sigma_-)$. The dashed detectors will observe no intensity correlation. Additional FRFT systems are used so that the total propagation for signal and idler is characterized by FRFTs of orders $\alpha_s=\alpha_{\mathrm{sep}}+\alpha_{s2}$ and $\alpha_i=\alpha_{\mathrm{sep}}+\alpha_{i2}$, respectively. Intensity correlation is recovered for any α_{s2} and α_{i2} such that $\alpha_i+\alpha_s(\mathrm{mod}2\pi)=0$.

ity will be satisfied, because the real part of the wave function becomes separable and the entanglement is present only in the imaginary part. An analysis similar to that of Ref. [17] in terms of FRFTs yields a separability condition for the real part of the wave function (1) given by $\alpha_{\mathrm{sep}}=\tan^{-1}(\sigma_+\sigma_-)$, where $\alpha_s=\alpha_i=\alpha_{\mathrm{sep}}$ is the order of the FRFT implemented on both fields. Substituting this condition in Eq. (7) shows that the DGCZ inequality is not violated.

To successfully detect entanglement in this case, it is necessary to adopt a scheme such as the one shown in Fig. 3. Signal and idler fields propagate through optical systems characterized by FRFTs of order α_{sep}, so that the separability condition for the real part of the wave function is reached. At this point, intensity correlations alone will fail to register entanglement. To detect entanglement, additional optical systems are used to implement a second FRFT in the signal and idler beams, with orders α_{s2} and α_{i2}, respectively. The optical systems can be designed so that the additivity of two consecutive FRFTs is preserved [19]. The signal beam has had a total propagation characterized by a FRFT of order $\alpha_s=\alpha_{\mathrm{sep}}+\alpha_{s2}$ and the idler $\alpha_i=\alpha_{\mathrm{sep}}+\alpha_{i2}$. In this case, applying the condition $\alpha_i+\alpha_s(\mathrm{mod}2\pi)=0$, Eq. (6) shows that the DGCZ inequality will be violated in the same way as it would be for the field in the source.

In conclusion, we have demonstrated theoretically and experimentally that it is possible to detect transverse entanglement performing intensity correlation measurements, not only in the near and far fields but also at intermediate propagation planes. This is achieved using optical systems that implement FRFTs according to the condition $\alpha_s+\alpha_i=2n\pi$, where α_s and α_i are the orders of the transforms on the signal and idler fields. We also show that entanglement is never registered when $\alpha_i+\alpha_s(\mathrm{mod}\pi)=\pi/2$. These results demonstrate that, given a signal field propagation characterized by α_s, one can always find an FRFT α_i that can be used to detect entanglement with intensity correlations alone. Though our experiment was conducted using spatial entanglement of photons, our results are directly applicable to spatial entanglement in other systems [15,16]. Since the fractional Fourier transform describes rotation in phase space, our results are applicable to a number of physical systems.

Financial support was provided by Brazilian agencies CNPq, PRONEX, CAPES, FAPERJ, FUJB, and the Milenium Institute for Quantum Information.

[1] *The Physics of Quantum Information*, edited by D. Bouwmeester, A. Ekert, and A. Zeilinger (Springer-Verlag, Berlin, 2000).
[2] P. G. Kwiat, K. Mattle, H. Weinfurter, A. Zeilinger, A. V. Sergienko, and Y. Shih, Phys. Rev. Lett. **75**, 4337 (1995).
[3] P. R. Tapster, J. G. Rarity, and P. C. M. Owens, Phys. Rev. Lett. **73**, 1923 (1994).
[4] A. Vaziri, G. Weihs, and A. Zeilinger, Phys. Rev. Lett. **89**, 240401 (2002).
[5] J. C. Howell, R. S. Bennink, S. J. Bentley, and R. W. Boyd, Phys. Rev. Lett. **92**, 210403 (2004).
[6] M. D'Angelo, Y.-H. Kim, S. P. Kulik, and Y. Shih, Phys. Rev. Lett. **92**, 233601 (2004).
[7] P. H. S. Ribeiro, S. Pádua, J. C. M. da Silva, and G. A. Barbosa, Phys. Rev. A **49**, 4176 (1994).
[8] D. V. Strekalov, A. V. Sergienko, D. N. Klyshko, and Y. H. Shih, Phys. Rev. Lett. **74**, 3600 (1995).
[9] A. F. Abouraddy, B. E. A. Saleh, A. V. Sergienko, and M. C. Teich, Phys. Rev. Lett. **87**, 123602 (2001).
[10] W. A. T. Nogueira, S. P. Walborn, S. Pádua, and C. H. Monken, Phys. Rev. Lett. **86**, 4009 (2001).
[11] L.-M. Duan, G. Giedke, J. I. Cirac, and P. Zoller, Phys. Rev. Lett. **84**, 2722 (2000).
[12] S. Mancini, V. Giovannetti, D. Vitali, and P. Tombesi, Phys. Rev. Lett. **88**, 120401 (2002).
[13] H. Bechmann-Pasquinucci and W. Tittel, Phys. Rev. A **61**, 062308 (2000).
[14] D. Collins, N. Gisin, N. Linden, S. Massar, and S. Popescu, Phys. Rev. Lett. **88**, 040404 (2002).
[15] M. V. Fedorov, M. A. Efremov, A. E. Kazakov, K. W. Chan, C. K. Law, and J. H. Eberly, Phys. Rev. A **72**, 032110 (2005).
[16] L. Lamata, J. J. García-Ripoll, and J. I. Cirac, Phys. Rev. Lett. **98**, 010502 (2007).
[17] K. W. Chan, J. P. Torres, and J. H. Eberly, Phys. Rev. A **75**, 050101(R) (2007).
[18] W. H. Peeters, E. J. K. Verstegen, and M. P. van Exter, Phys. Rev. A **76**, 042302 (2007).
[19] H. M. Ozaktas, Z. Zalevsky, and M. A. Kutay, *The Fractional Fourier Transform, with Applications in Optics and Signal Processing* (Wiley, New York, 2000).
[20] A. W. Lohmann, J. Opt. Soc. Am. A **10**, 2181 (1993).
[21] P. Pellat-Finet and G. Bonnet, Opt. Commun. **111**, 141 (1994).
[22] D. S. Tasca, F. Toscano, S. P. Walborn, and P. H. S. Ribeiro (unpublished).
[23] P. Pellat-Finet, Opt. Lett. **19**, 1388 (1994).
[24] In general, this phase term can be removed by considering propagation to a spherical surface, and higher-order FRFT's can be defined by free propagation between sets of spherical emitters and receivers [21,23].